Effect of *n*-butanol and diethyl ether as oxygenated additives on combustion–emission-performance characteristics of a multiple cylinder diesel engine fuelled with diesel–jatropha biodiesel blend

S. Imtenan *, H.H. Masjuki *, M. Varman, I.M. Rizwanul Fattah *, H. Sajjad, M.I. Arbab

Centre for Energy Sciences, Department of Mechanical Engineering, Faculty of Engineering, University of Malaya, 50603 Kuala Lumpur, Malaysia

ARTICLE INFO

Article history:
Received 1 November 2014
Accepted 18 January 2015
Available online 7 February 2015

Keywords:
Diesel–biodiesel blend
n-Butanol
Diethyl ether
Combustion
Engine performance-emission

ABSTRACT

Jatropha biodiesel is considered as one of the most prospective renewable energy sources of Malaysia in recent years. Hence, an investigation was conducted for the improvement of jatropha biodiesel–diesel blend with the addition of 5–10% *n*-butanol and diethyl ether by vol. which are commonly known as oxygenated cold starting additive. Engine tests were conducted at variable speed, ranging from 1000 rpm to 3000 rpm at constant 80 N m torque on a 4-cylinder turbocharged indirect injection diesel engine. Engine performance parameters like brake specific fuel consumption, brake specific energy consumption, brake thermal efficiency and engine emissions like carbon monoxide, unburned hydrocarbons, nitrogen oxide and smoke opacity were measured. Performance and exhaust emissions variation of the modified blends from the baseline fuel (jatropha biodiesel–diesel blend) were compared for the assessment of the improvement quantitatively. In-cylinder pressure diagram of all the test fuels were acquired and the heat release rate analysis was conducted at different operating conditions to explore the features of combustion mechanism and correlate them with the performance and emission characteristics to acquire better understanding of the scenario. However, in a nut-shell, the investigation reveals the potential of *n*-butanol and diethyl ether to be used as the additive of jatropha biodiesel–diesel blend in the context of combustion, performance and emission characteristics.

1. Introduction

Biodiesel refers to the fatty acid methyl esters which are derived from lipid substances from oils, fats, waste greases, recycled oils, etc. To produce biodiesel, vegetable oils of edible origin were treated as one of the potential feedstocks once. Due to food vs. fuel controversy of usage of edible oil for fuel production, other sources e.g. non-edible oils of plant origin with high free fatty acid (FFA) content, etc. are now being used for biodiesel production. Malaysia is one of the leading palm oil producers in the world [1]. In addition, it also facilitates the use of palm oil as fossil diesel replacement. The government of Malaysia has recently mandated the use of 5% palm biodiesel with diesel nationwide for all diesel vehicle [2]. However, because of the edible nature of the palm oil, recently jatropha has drawn immense attention of both private and government sectors in Malaysia. *Jatropha curcas* is non-edible in nature, physicochemical properties of its biodiesel are quite similar to the palm biodiesel and most interestingly, it has been reported as one of the best contestants of cheap biodiesel source in future [3]. Hence, Malaysian government started a project concerning jatropha cultivation and economic viability study of jatropha biodiesel production [4]. It has been reported that, Forest Research Institute of Malaysia (FRIM) has completed a 6000 *J. curcas* tree plantation project and the agency has confirmed that it is ready to proceed to commercial scale [5]. Therefore, being a prospective non-edible renewable energy source with satisfactory physicochemical properties, jatropha biodiesel deserves profound investigation regarding its viability in the diesel engines.

Many experiments were done with neat jatropha biodiesel or its blends with diesel to study their effects on engine performance and emission characteristics. Huang et al. [6] studied with jatropha biodiesel and reported 3.6% higher brake thermal efficiency (BTE) compared to diesel at higher loads in expense of higher brake specific fuel consumption (BSFC). Sundaresan et al. [7] also found from their study that the engine efficiency and BSFC for jatropha were inferior to that of diesel fuel. However, pre-heating and blending

* Corresponding authors. Tel.: +60 146985294; fax: +60 3 79675245 (S. Imtenan). Tel.: +60 3 79675245; fax: +60 3 79675245 (H.H. Masjuki). Tel.: +60 3 79674448; fax: +60 3 79675245 (I.M. Rizwanul Fattah).

E-mail addresses: sayeed.imtenan@gmail.com (S. Imtenan), masjuki@um.edu.my (H.H. Masjuki), rizwanul.buet@gmail.com (I.M. Rizwanul Fattah).

http://dx.doi.org/10.1016/j.enconman.2015.01.047
0196-8904/

with diesel have been reported conducive for engine performance characteristics [8]. Manieniyan and Sivaprakasam [9] reported significant improvement of performance while they tried 20% blend of jatropha biodiesel which was also supported by the work of Sahoo et al. [10]. Therefore, blending with petroleum diesel as a single biodiesel [11] or as an optimized multiple biodiesel blend [12] have already been studied by several researchers.

The problems associated to biodiesel is its high viscosity and auto ignition temperature (AIT) compared to that of diesel. To minimize these drawbacks as well as to increase the fuel bound oxygen (to facilitate combustion) and to keep lubricity at reasonable levels, oxygenated additives such as *n*-butanol and diethyl ether (DEE) are usually added in a small portion [13]. *n*-butanol has emerged as a potential oxygenated additive to improve the fuel properties of both diesel and biodiesels recently. *n*-butanol, also better known as 1-butanol, is produced from alcoholic fermentation of biomass feedstocks [14]. Hence, it is a renewable additive with a straight-chain structure with the OH group at the terminal carbon. *n*-butanol is a strong competitor of ethanol and has less hydrophilic tendency, higher cetane number, higher miscibility with diesel and biodiesels and higher calorific value [15]. Yao et al. [16] investigated the influence of *n*-butanol-diesel blend on the performance and emissions of a heavy-duty diesel engine with multi-injection and various EGR (exhaust gas recirculation) ratios. They reported that, the soot and CO emissions can be improved by the addition of *n*-butanol without a severe impact on the BSFC. Altun et al. [17] studied the effect of *n*-butanol on cottonseed biodiesel–diesel blend and reported that, emissions of NO_x, HC and CO reduced in expense of higher BSFC. Lebedevas et al. [18] experimented with butyl esters of rapeseed oil-diesel blend with the addition of 15–25% *n*-butanol and reported improvement on emission characteristics and overall efficiency factor. In their study, Mehta et al. [19] studied the effect of varying percentage of *n*-butanol with jatropha biodiesel–diesel blend and reported significant reduction in CO and NO emission in expense of lower engine performance. However, they did not analyse their data with sufficient insight on combustion phenomena at each condition. Thus, the disadvantage of higher viscosity of biodiesel and the lower cetane number of *n*-butanol than biodiesel can be offsetted with the addition of *n*-butanol as additive.

Diethyl ether is another biomass based oxygenated additive produced from ethanol, which is produced itself from biomass [20]. It is a colorless liquid with high volatility and flammability. It has got very high cetane number, reasonable energy density and low AIT with high oxygen content. It has high miscibility with both diesel and biodiesel. Consequently, it is very much suitable to be used in diesel engine either with diesel or biodiesels [21]. Many researchers have studied diesel-DEE blend to improve the performance and emission characteristics. Blending with neat biodiesel or biodiesel–diesel blend has also been tried by the researchers. Babu et al. [22] evaluated the effect of DEE on mahuva methyl ester and reported that, CO and smoke emission decreased more than 50% after addition of DEE. Sivalaksmi and Balusamy [23] added 5–15% DEE on neat neem biodiesel and reported improvement of BSFC and BTE. Qi et al. [24] studied effect of 5% DEE addition with soybean biodiesel–diesel blend. They observed significantly lower CO emission with better BSFC with the addition of DEE into the diesel–biodiesel blend. Thus, it can be concluded that, addition of DEE results in improved performance and emission characteristics of diesel engines.

Jatropha biodiesel has the potential to be used as partial replacement of diesel in Malaysia after palm oil. Therefore, an attempt was taken previously by the authors for the improvement with the addition of *n*-butanol and DEE [4]. On that investigation it was observed that addition of 5% *n*-butanol and DEE improved the brake power (3.5%), brake thermal efficiency (3.4%) and also reduced the emissions of NO_x (9%), CO (20%) and smoke opacity (22%) of the modified blends than J20 blend on average with an unmodified single cylinder diesel engine. Apart from that, there is an absence of comparative study in the literature on the effects of higher percentages of *n*-butanol and DEE as additives on jatropha biodiesel–diesel blends on multiple cylinder engines. Therefore, in the present investigation the authors have attempted to increase the percentage of *n*-butanol and DEE in the quest of studying the effects in a four cylinder, water cooled turbocharged diesel engine. In addition, combustion analysis has been incorporated at different operating conditions to get in-depth understanding of the combustion mechanisms and their correlation with the performance and emission characteristics. Cost analysis of all the modified blends have also been incorporated into this study to provide an economic comparison of different tested fuels.

2. Materials and method

2.1. Feedstock and additive

FRIM (Forest Research Institute Malaysia) supplied the jatropha biodiesel. *n*-butanol and DEE were purchased from Nacalai Tesque, Inc., Kyoto, Japan; certified as 99.5% pure. Petroleum diesel was supplied from the local market supplier.

2.2. Fatty acid composition (FAC)

In this investigation Shidmadzu, GC-2010A series gas chromatograph was used to explore the FAC of jatropha biodiesel. Tables 1 and 2 show the GC operating conditions and the FAC results of the biodiesel. Jatropha biodiesel contains 24.3% saturated, 42.6% mono-unsaturated and 33.1% poly-unsaturated methyl esters. Higher portion of saturation indicates higher oxidation stability and CN (cetane number). On the contrary it also indicates lower iodine value and CFPP according to the literature review [25].

2.3. Test fuels

The preparation of the test fuels and characterization of the properties were carried out at the Engine Tribology Laboratory, Department of Mechanical Engineering, University of Malaya. A total of six test fuels were selected for this investigation. The test fuels were (a) 100% petroleum diesel, (b) 20% Jatropha biodiesel + 80% diesel (J20), (c) 15% Jatropha biodiesel + 5% *n*-butanol + 80% diesel (J15B5), (d) 10% Jatropha biodiesel + 10% *n*-butanol + 80% diesel (J10B10), (e) 15% Jatropha biodiesel + 5% DEE + 80% diesel (J15D5), (f) 10% Jatropha biodiesel + 10% DEE + 80% diesel (J10D10). The proportions mentioned here were all volume based. Diesel and biodiesel blending was completed

Table 1
GC operating condition for determination of fatty acid composition.

Item	Specification
Column	0.32 mm * 30 m, 0.25 μm
Injection volume	1 μm
Carrier gas	Helium, 83 kPa
Injector	Split/splitless 1177, full EFC control
Temperature	250 °C
Split flow	100 mL/min
Column 2 flow	Helium at 1 ml/min constant flow
Oven	210 °C isothermal
Column temperature	60 °C for 2 min 10 °C/min to 200 °C 5 °C/min to 240 °C Hold 240 °C for 7 min
Detector	250 °C, FID, full EFC control

Table 2
Fatty acid composition of biodiesels.

FAME	Structure	Molecular weight	Formula	JBD (wt.%)
Methyl laurate	12:00	214.34	$CH_3(CH_2)_{10}COOCH_3$	0
Methyl myristate	14:00	242.4	$CH_3(CH_2)_{12}COOCH_3$	0.1
Methyl palmitate	16:00	270.45	$CH_3(CH_2)_{14}COOCH_3$	17.7
Methyl palmitoleate	16:01	268.43	$CH_3(CH_2)_5CH{=}CH(CH_2)_7COOCH_3$	0.8
Methyl stearate	18:00	298.5	$CH_3(CH_2)_{16}CO_2CH_3$	6.4
Methyl oleate	18:01	296.49	$CH_3(CH_2)_7CH{=}CH(CH_2)_7COOCH_3$	41.8
Methyl linoleate	18:02	294.47	$CH_3(CH_2)_3(CH_2CH{=}CH)_2(CH_2)_7COOCH_3$	32.9
Methyl linolenate	18:03	292.46	$CH_3(CH_2CH{=}CH)_3(CH_2)_7COOCH_3$	0.2
Methyl archidate	20:00	326.56	$CH_3(CH_2)_{18}COOCH_3$	0.1
Methyl eicosenoate	20:01	324.54	$CH_3(CH_2)_{16}CH{=}CHCOOCH_3$	0
Methyl behenate	22:00	354.61	$CH_3(CH_2)_{20}COOCH_3$	0
Methyl lignocerate	24:00	382.66	$CH_3(CH_2)_{22}COOCH_3$	0
Saturation				24.3
Mono-unsaturation				42.6
Poly-unsaturation				33.1
Unsaturation				75.7

by a blending machine at 4000 rpm for 15–20 min. As *n*-butanol and DEE are volatile in nature, after addition of *n*-butanol and DEE, the blends were taken into a closed container and shaked with a shaker machine for about 30 min.

2.4. Equipment for fuel property test

Table 3 shows the list of the equipment used to measure the physicochemical properties of the base fuels (diesel and biodiesels) and fuel blends. The following equations were used to calculate the saponification number (SN), iodine value (IV) and cetane number (CN) of the biodiesel [25].

$$SN = \sum\left(\frac{560 \times Ai}{MWi}\right) \quad (1)$$

$$IV = \sum\left(\frac{254 \times D \times Ai}{MWi}\right) \quad (2)$$

$$CN = 46.3 + \left(\frac{5458}{SN}\right) - (0.225 \times IV) \quad (3)$$

Here, A_i = percentage of each component, D = number of double bonds, MW_i = mass of each component. Molecular weight of each component is given in Table 2.

2.5. Fuel properties

Tables 4 and 5 show the physicochemical properties of the base fuels and the blends respectively. Each property was tested several times and then mean value was taken.

Kinematic viscosity of the biodiesels depends on the fatty acid profile [28]. Table 4 shows that, kinematic viscosity of the jatropha biodiesel satisfies the ASTM-D6751 and EN 14214 standards. Though jatropha biodiesel is meeting the standard, still it is 15% higher than the diesel fuel. From Table 5 it can be seen that, addition of *n*-butanol and DEE reduced the value of kinematic viscosities of the modified blends at best 26%. All the blends meet the ASTM D7467 standard of viscosity. Lower kinematic viscosity is supposed to assist the modified blends to get better atomization during the injection than the J20 blend.

Density of the jatropha biodiesel was 3.4% higher than diesel fuel. However, blending with diesel (J20) reduced the density to some extent. Compared to J20, *n*-butanol and DEE blends showed further reduction. Up to 4.4% reduced density was observed for the modified blends than J20. Increasing portion of *n*-butanol and DEE reduced the density accordingly which made the values much similar to diesel fuel.

The calorific value of jatropha biodiesel was lower than diesel as expected. On top of that, calorific values of *n*-butanol and DEE were even lower than the biodiesel. Consequently, all the blends J20, J15B5, J10B10, J15D5 and J10D10 showed lower calorific values than diesel, yet the values were only 2.95% lower on average than diesel.

Flash point of the jatropha biodiesel was very much higher than diesel fuel, which is positive in terms of transportation and handling. Flash points of *n*-butanol and DEE were very low, therefore modified blends showed quite lower flash points than J20. However, generally a flash point higher than 66 °C is considered as safe [29] and on top all the modified blends satisfy the ASTM D7467 standard for flash point. Therefore, in this study it can be said that all the fuels were safe to handle.

The cloud point and pour point values are of limited concern in tropical and hot countries of Asia, but it has much greater importance in countries where the weather is cold. It can be seen from Table 4 that cloud point and pour point of jatropha biodiesel was quite higher than the diesel. However, as the *n*-butanol and DEE

Table 3
Equipment of fuel property test.

Property	Equipment	Manufacturer	Standard method	ASTM D6751 limit	Accuracy
Kinematic viscosity at 40 °C	SVM 3000-automatic	Anton Paar, UK	D7042	1.9–6.0	±0.35%
Density at 40 °C	SVM 3000-automatic	Anton Paar, UK	D7042	n.s.	0.0005 g/cm3
Flash point	Pensky–Martens flash point-automatic NPM 440	Normalab, France	D93	130 min	±0.1 °C
Oxidation stability	873 Rancimat-automatic	Metrohm, Switzerland	EN 14112	3 h	±0.01 h
Higher heating value	C2000 basic calorimeter-automatic	IKA, UK	D240	n.s.	±0.1% of reading
Cloud point	Cloud and Pour point tester-automatic NTE 450	Normalab, France	D2500	Report	±0.1 °C
Pour point	Cloud and Pour point tester-automatic NTE 450	Normalab, France	D97		±0.1 °C
CFPP	Cold filter plugging point-automatic NTL 450	Normalab, France	D6371	n.s.	
Acid value	G-20 Rondolino automated titration system	Mettler Toledo, Switzerland	D664	0.5 max	±0.001 mg KOH/g

Table 4
Property of the base fuels.

Property	Unit	Diesel	JBD	*n*-butanol[c]	Diethyl ether[c]	ASTM D6751[a]	EN 14214[b]
Kinematic viscosity at 40 °C	mm^2/s	3.46	4.27	3.00	0.22	1.9–6.0	3.5–5.0
Density at 40 °C	kg/m^3	833	861	812	712	n.s.	n.s.
Lower heating value	MJ/kg	44.66	39.83	34.33	33.89	n.s.	n.s.
Oxidation stability	h	59.10	3.11	–		3 (min)	6 (min)
Flash point	°C	69.5	202.5	35	−40	130 (min)	120 (min)
Cloud point	°C	8	3			report	n.s.
Pour point	°C	7	2	−89	–	n.s.	n.s.
CFPP	°C	8	8			n.s.	n.s.
Acid value	Mg KOH/g	–	0.18	–		0.5 (max)	0.5 (max)
Saponification number (SN)			192.6	–		n.s.	n.s.
Iodine value (IV)	G I_2/100 g		93.8	–		n.s.	120
Cetane number (CN)		48	53.5	25	~125	47 (min)	51 (min)

n.s. = not specified.
[a] Data obtained from [26].
[b] Data obtained from [27].
[c] Provided by the supplier, measured at 20 °C.

Table 5
Property of the fuel blends.

Property	Diesel	J20	J15B5	J10B10	J15D5	J10D10	ASTM D7467
Kinematic viscosity at 40 °C	3.46	3.60	3.29	3.24	3.22	3.15	1.9–4.1
Density at 40 °C	833	837	834	831	830	823	n.s.
Lower heating value							
MJ/kg	44.66	43.69	43.40	43.15	43.39	43.10	n.s.
Flash point °C	69.5	96.5	87.5	79.5	83.5	71.5	52 (min)

are well accepted as the cold starting additives, it is not necessary to measure the cloud point and pour point of the modified blends [30].

2.6. Experimental setup

This investigation was performed using an inline four-cylinder, water-cooled, turbocharged diesel engine without any catalytic converter. Schematic diagram of the test setup is given in Fig. 1. Engine specifications are listed in Table 6. An eddy current dynamometer, which can be operated at a maximum power of 250 kW was coupled to the engine. Measurement of HC, NO and CO emissions were conducted by Bosch BEA-350 exhaust gas analyzer. Smoke opacity was measured by Bosch RTM 430 smoke opacimeter. The method for measuring the HC and CO emissions was Non-dispersive infrared and the method for NO was electrochemical. Smoke opacity was measured by photodiode receiver method.

Engine performance and emission tests were carried out varying the engine speed ranging from 1000 to 3000 rpm at constant 80 N m torque. For data acquisition, REO-DEC data control system was used, which was monitored with the help of REO-DCA software. Measured engine performance parameters of this investigation were BSFC (brake specific fuel consumption), BSEC (brake specific energy consumption) and BTE (brake thermal efficiency).

2.7. Combustion characteristics analysis

The test system was equipped with necessary sensors for combustion analysis. In-cylinder pressure was measured by using a

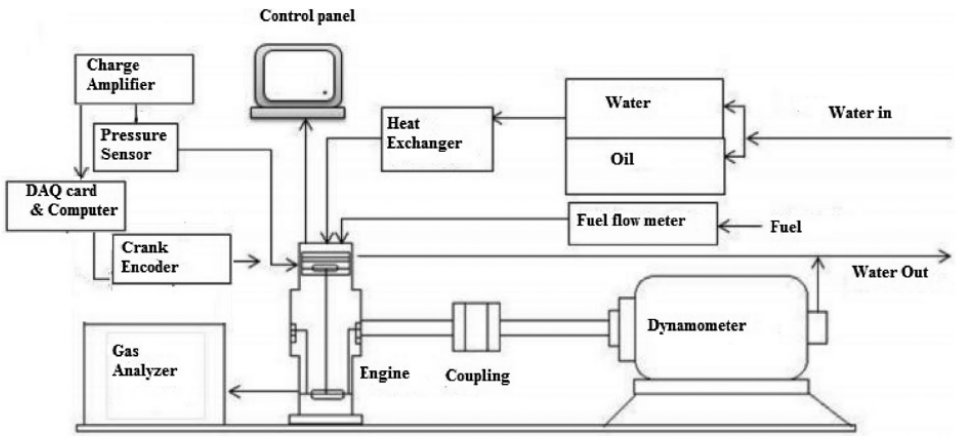

Fig. 1. Schematic diagram of the engine test bed.

Table 6
Engine testbed equipment specification.

Description	Specification
No. and arrangement of cylinders	4 in-line, longitudinal
Rated power	65 kW at 4200 rpm
Combustion chamber	Swirl chamber
Total displacement	2477 cc
Cylinder bore × stroke	91.1 × 95 mm
Valve mechanism	SOHC
Compression ratio	21:1
Lubrication system	Pressure feed, full flow filtration
Fuel system	Distributor type injection pump
Air flow	Turbocharged
Fuel injection pressure	157 bar
Dynamometer	Froude Hofmann eddy current dynamometer Max. Power: 250 kW Max. Torque: 1200 N m Max. Speed: 6000 rpm
Fuel flow meter	Positive displacement flow meter

Kistler 6058A type pressure sensor. It was installed in the swirl chamber through the glow plug port. Kistler 2614B4 type charge amplifier was used to amplify the charge signal outputs from the pressure sensor. A high precision incremental encoder (2614A type) was used to acquire the top dead center (TDC) position and crank angle signal for every engine rotation. Simultaneous samplings of the cylinder pressure and encoder signals were performed by a computer with Dewe-30-8-CA data acquisition card. One hundred consecutive combustion cycles of pressure data were collected and averaged to eliminate cycle-to-cycle variation in each test. To reduce noise effects, Savitzky–Golay smoothing filtering was applied to the sampled cylinder pressure data. Other combustion parameters, such as heat release rate and start of combustion (SOC) were computed by using Matlab® R2009a software.

Heat release rate (HRR) analysis is the most effective way to gather information for the combustion mechanism in diesel engines. This method simplifies the identification of start of combustion (SOC) timing and differences in combustion rates from the HRR versus crank angle diagram [31]. Hence, HRR analysis is a significant parameter in understanding the combustion mechanism. Average in-cylinder pressure data of 100 consecutive cycles with a 0.1 crank angle (CA) resolution were used to calculate HRR. Analysis was derived from the first law of thermodynamics, as shown in Eq. (4), without taking into account heat loss through cylinder walls. Here, main combustion chamber and pre-combustion chamber were considered to be combined into a single zone thermodynamic model. It is expected that, in between the two chambers, there is no passage throttling losses. Fuel vaporization and mixing, temperature gradients, non-equilibrium conditions and pressure waves can be ignored [32].

$$\frac{dQ}{d\theta} = \frac{V\frac{dP}{d\theta} + \gamma P\frac{dV}{d\theta}}{\gamma - 1} \tag{4}$$

where $\frac{dQ}{d\theta}$ = rate of heat release (J/°CA), V = instantaneous cylinder volume (m^3), θ = crank angle (°CA), P = instantaneous cylinder pressure (Pa), γ = specific heat ratio which is considered constant at 1.35 [33]. The input values are the pressure data and cylinder volume (with respect to crank angle). The V and $\frac{dV}{d\theta}$ terms are shown in the following equations:

$$V = V_c + A \cdot r\left[1 - \cos\left(\frac{\pi\theta}{180}\right) + \frac{1}{\lambda}\left\{1 - \sqrt{1 - \lambda^2 \sin^2\left(\frac{\pi\theta}{180}\right)}\right\}\right] \tag{5}$$

Table 7
Measurement accuracy and uncertainty.

Measured quantity	Upper limit	Accuracy	Uncertainty (%)
Fuel flow	36 l/h	±0.02 l/h	–
Speed	6000 rpm	±2 rpm	–
Power	250 kW	±0.02 kW	–
Smoke opacity	100%	0.1%	±0.5%
CO	10.00 vol%	0.02 vol%	±0.01 vol%
HC	9999 ppm vol	1 ppm vol	±1 ppm
NO	5000 ppm vol	1 ppm vol	±5 ppm

$$\frac{dV}{d\theta} = \left(\frac{\pi A}{180}\right) \times r\left\{\sin\left(\frac{\pi\theta}{180}\right) + \frac{\lambda^2 \sin^2\left(\frac{\pi\theta}{180}\right)}{2 \times \sqrt{1 - \lambda^2 \sin^2\left(\frac{\pi\theta}{180}\right)}}\right\} \tag{6}$$

Here, $\lambda = \frac{l}{r}$ and $A = \frac{\pi D^2}{4}$, where l = connecting rod length, r = crank radius = 0.5 × stroke, D = cylinder bore, and V_c = clearance volume.

2.8. Accuracies and uncertainties

Uncertainty in the measurements may happen due to experimental conditions, equipment calibration, instrument selection and inaccuracies. Therefore, it is much needed to analyze the uncertainty of the measured values. Uncertainty of this experiment was analyzed through a study of the instruments' precision and accuracy (given in Table 7) along with the repeatability of the tests using the similar method by Fattah et al. [34]. Experiments were performed several times, and data were collected at least three times. Average values were used for graph plotting.

3. Results and discussions

3.1. Combustion characteristics

3.1.1. Analysis of in-cylinder pressure

The parameters used to compare the combustion characteristics in this investigation were cylinder gas pressure, start of combustion (SOC) and heat release rate (HRR). With focus on the 'hot' part around TDC (top dead center), cylinder pressure against crank angle diagram for jatropha biodiesel blend and its modified blends with *n*-butanol are illustrated in Fig. 2 at 1000, 2000 and 3000 rpm keeping the toque constant at 80 N m. It can be seen from the figure that, there were no significant differences on the maximum in-cylinder pressures among the fuels. Such result actually replicates that, conversion of fuel energy into mechanical energy was as efficient for the modified blends as for the diesel fuel [32].

However, for J20 and its modified blends with additives, maximum in-cylinder pressure occurred after top dead center (ATDC) within the range of 8–10.5° CA. It can be seen from Fig. 2 that, as the speed increased, in-cylinder pressure increased accordingly. Up to 2000 rpm, J20 showed higher maximum in-cylinder pressure than diesel. Higher and slight early maximum pressure for the J20 blend can be attributed to the higher cetane number of the jatropha biodiesel compared to diesel [4]. However, at 3000 rpm, maximum pressure for J20 was lower compared to diesel. Poor atomization and air–fuel mixing due to higher density, viscosity of J20 and less available time due to higher speed resulted reduced premixed charge. Consequently peak in-cylinder pressure reduced [23]. With the addition of *n*-butanol into the jatropha biodiesel-diesel blend, it was observed that the peak cylinder pressure decreased and occurred a bit late at all the observed engine speeds. At 3000 rpm, J15B5 and J10B10 produced 86.95 bar and 86.07 bar of maximum in-cylinder pressures respectively at 9.4° ATDC and 9.9° ATDC. Crank angles for the maximum pressures of these two

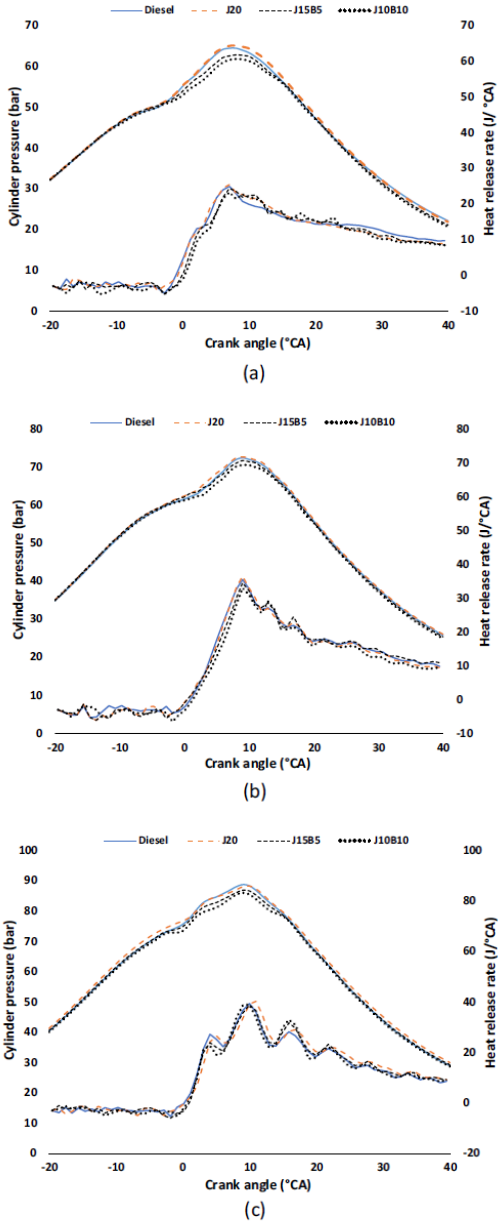

Fig. 2. Cylinder pressure and heat release rate vs crank angle diagram for *n*-butanol blends at (a) 1000 rpm, (b) 2000 rpm and (c) 3000 rpm.

blends were almost similar at the other engine speeds. Descending pressures with the increment of the percentage of *n*-butanol can be explained by lower calorific value of the *n*-butanol compared to diesel and biodiesels [35].

Fig. 3 shows the in-cylinder pressure against crank angle diagram for jatropha biodiesel blend and its modified blends with DEE at different engine speed. Similar to *n*-butanol blends, addition of DEE reduced the maximum in-cylinder pressure. At 3000 rpm, Maximum in-cylinder pressures for J15D5 and J10D10 were observed 86.92 and 86.10 bar respectively at 10.1° ATDC and 10.4° ATDC. Slight late and lower maximum in-cylinder pressures for the DEE blends can be explained more clearly by combining it to the HRR analysis of the corresponding fuels.

3.1.2. Analysis of heat release rate

Heat release rate analysis is one of the finest tools to get in-depth understanding of the combustion phenomena in an engine. In-cylinder pressure characteristics of the fuels can be explained in a better way conjoining the HRR analysis. In the present study, the engine has a pump-line-nozzle fuel injection system and advanced start of injection (SOI) can take place if the fuel is denser and has higher bulk modulus of compressibility (and vice versa). Therefore, instead of measuring the ignition delay, in this study combustion scenario is described with the help of SOCs (start of combustion). In this investigation, SOCs were acquired from the HRR against crank angle diagram. Theoretically, as the piston is near the TDC, fuel vaporization causes a negative heat release and with the start of combustion, heat release momentarily becomes positive at a point. This point is called SOC.

Heat release rate of the jatropha biodiesel blend and its modified blends with *n*-butanol are given in the Fig. 2 at different speed. It can be seen in the figure that, at 1000 and 2000 rpm, premixed combustion (area under the first sharp peak in the HRR diagram) of the J20 blend was quite higher than the diesel fuel, which actually led to a little higher maximum pressure for this fuel [23]. However, at 3000 rpm, premixed part of the combustion was lower for J20 than diesel, which reflected slight lower in-cylinder peak pressure discussed earlier. At 3000 rpm, SOC of the J20 was observed at -3.7°ATDC while at 1000 and 2000 rpm SOCs were almost same at -4°ATDC. It actually demonstrates that J20 encountered difficulties regarding proper atomization and consequently at higher speed, higher crank angle revolution was needed to make the charge combustible.

With the addition of *n*-butanol, it was detected that J15B5 and J10B10 got late SOCs compared to J20 and diesel at all the observed engine speeds. SOC of J15B5 was observed on -3.9°ATDC whereas for J10B10 it was on -3.5°ATDC on average regarding the 1000, 2000 and 3000 rpm. Similarly, from Fig. 3 it can be seen that SOCs of J15D5 and J10D10 were at -3.7°ATDC and -3.1°ATDC on average regarding the observed engine speeds respectively. Since, *n*-butanol has a lower cetane number, SOC occurred late for comparatively higher ignition delay [36]. On the contrary, despite of higher cetane number of DEE, SOCs of DEE blends retarded due to its higher latent heat of evaporation which is supported by the work of Rakopoulos [13]. Such offset of SOCs were translated into comparatively lower maximum in-cylinder pressures both for *n*-butanol and DEE blends. Since the SOCs were late, it was more likely that combustion occurred in a lower temperature environment, consequently lowered the peak pressures. However, it can be seen that, 10% blends of the additives got more retarded SOCs compared to 5% blends of the additives. Since, current investigation was conducted in a turbocharged engine; fuel–air ratio was very low. Therefore, it is evident that, effect of lower temperature during the vaporization of the fuel was not significant enough for the 5% blends of *n*-butanol and DEE. However, 10% *n*-butanol and DEE helped to create significantly lower temperature during the vaporization of the fuel and delayed the SOCs more. However, in the mixing controlled zone (area after the first sharp peak) both of the modified blends exhibited higher HRR than J20, which actually indicates better atomization of fuel due to lower density and viscosity of *n*-butanol and DEE [13].